

# Magnetostatic interaction in arrays of nanometric permalloy wires: A magneto-optic Kerr effect and a Brillouin light scattering study

G. Gubbiotti\*

*Research Center SOFT-INFN-CNR, Università di Roma "La Sapienza," I-00185, Roma, Italy*

S. Tacchi

*Dipartimento di Fisica, Università di Perugia, Via A. Pascoli, 06123 Perugia, Italy*

G. Carlotti

*INFN-CNR Research Center S3, Via Campi 213/a, 41100, Modena, Italy  
and Dipartimento di Fisica, Università di Perugia, Via A. Pascoli, 06123 Perugia, Italy*

P. Vavassori

*INFN-CNR Research Center S3, Via Campi 213/a, 41100, Modena, Italy  
and Dipartimento di Fisica, Università di Ferrara, Via G. Saragat 1, 44100 Ferrara, Italy*

N. Singh, S. Goolaup, and A. O. Adeyeye

*Information Storage Materials Laboratory, Department of Electrical and Computer Engineering, Engineering Drive 3,  
National University of Singapore 117576, Singapore*

A. Stashkevich

*LPMTM, Institut Galilée, Université Paris 13, 99 Avenue J.-B. Clément, 93430 Villetaneuse, France*

M. Kostylev

*St. Petersburg Electrotechnical University, 197376, St. Petersburg, Russia  
and School of Physics-M013, University of Western Australia, 35 Stirling Highway, Crawley, WA 6009, Australia  
(Received 28 July 2005; revised manuscript received 10 October 2005; published 9 December 2005)*

Two arrays of permalloy parallel wires, 20 nm thick, having the same width of 175 nm and different spacing of 35 and 175 nm were prepared by means of deep ultraviolet lithography and lift-off process. The effect of magnetostatic interaction on both the static and dynamic magnetic properties of arrays of wires has been investigated by means of magneto-optic and Brillouin light scattering techniques, respectively. In particular, the magnetization switching of the samples, measured by vectorial magneto-optical Kerr effect magnetometry and microscopy shows the effects of dipolar interaction in the case of 35 nm spaced wires, while in the other sample the measurements show that the wires are substantially noninteracting. The Brillouin light scattering measurements showed that for the sample with interwire spacing of 35 nm, dipolar coupling between magnetic wires leads to the formation of a collective mode which has a continuous spectrum and exists in a range of frequencies, while for the 175 nm spaced wires the spin modes are dispersionless. To quantify the investigated effects, a theory developed earlier for an isolated wire has been extended to the case of a one-dimensional array of ferromagnetic wires.

DOI: [10.1103/PhysRevB.72.224413](https://doi.org/10.1103/PhysRevB.72.224413)

PACS number(s): 75.75.+a, 76.50.+g, 78.35.+c

## I. INTRODUCTION

Advances in lithographic and other controlled fabrication techniques have recently given rise to the possibility of exploring magnetism in arrays of laterally controlled magnetic structures down to nanometer scales.<sup>1</sup> As a consequence, both static and dynamic behavior of nanopatterned magnetic structures has driven extensive research in recent years. Since minimizing the spatial separation of elements in data storage devices is a natural tendency, the magnetostatic interaction between magnetic elements has become a crucial key in controlling the magnetization reversal processes and the domain structures. Generally speaking, there is a large number of recently published papers where the effect of dipolar interactions becomes evident, mainly in the case of

nanometric systems.<sup>2-4</sup> However, it is rather difficult to produce arrays of magnetic elements with a very narrow distribution of shapes, sizes, and distances. Sometimes these statistical variations can hide the effects of magnetostatic interactions over arrays of hundreds of elements.

In arrays of well-separated magnetic wires and dots, the magnetization reversal is determined by the properties of individual elements, whereas interaction effects become essential when the interdot spacing is much smaller than the dot lateral sizes. In the case of nanodots, this leads to a considerable mutual influence between the dots during the magnetization reversal,<sup>5</sup> as well as to a magnetostatic coupling<sup>6</sup> between the dynamic modes of individual magnetic structures.<sup>7</sup> In the case of nanowires of a cylindrical cross

section, collective modes, due to the interplay between individual wires, were reported both in the theory<sup>8</sup> and in the experiment.<sup>9</sup> A slight interdot coupling was measured by Brillouin light scattering (BLS) in an array of circular permalloy dots (1  $\mu\text{m}$  diameter, 100 nm spacing). The in-plane frequency showed a twofold oscillation (of about 3%), reflecting the symmetry of the dot matrix, which was therefore attributed to the dipolar interaction between unsaturated parts of the dots.<sup>10</sup>

In a recent theoretical paper it was shown that due to inevitable dipolar coupling, collective modes are excited on periodic magnetic nanowires.<sup>16</sup> The magnetostatic coupling between the individual resonances produces two effects: a redistribution of the dynamic magnetization on each element and a corresponding frequency shift, which depends on the small wave number of the collective mode, thus the spin wave eigenexcitations of the array become dispersive waves.

To test the predictions of this theory and to gain further insights into the magnetostatic interaction, we studied a model system consisting of arrays of wires having different spacings. In this case, dipolar interwire coupling is relatively easy to interpret because, when uniformly magnetized along the easy direction, the wires can be well modeled as magnetic dipoles. This is not strictly true in the case of magnetic dots, which can develop complicated domains configurations to minimize surface charges.

## II. EXPERIMENT

Two arrays of 20 nm thick permalloy ( $\text{Ni}_{80}\text{Fe}_{20}$ ) nanowires with the same width,  $w=175$  nm and different spacings  $\Delta=35$  and 175 nm, were fabricated on a commercially available silicon substrate using deep ultraviolet lithography at 248 nm exposing wavelength. To create patterns in the resist, the substrate was coated with a 60 nm thick antireflective layer, followed by a 480 nm positive deep ultraviolet photoresist, which is 4 to 5 times thicker than those used in electron beam lithography. This allows the fabrication of nanowires with high aspect ratio and makes the lift-off process easier. A Nikon lithographic scanner with KrF excimer laser radiation was used for exposing the resist. To convert the resist patterns into nanowires, a 20 nm thick permalloy film was deposited using e-beam evaporation technique at a rate of 0.3  $\text{\AA}/\text{s}$ . The pressure was maintained at  $2 \times 10^{-6}$  Torr during deposition. Lift-off of the deposited film was carried out in OK73 solution and isopropyl alcohol (IPA). Completion of the lift-off process was determined by the color contrast of the patterned area ( $4 \times 4$  mm<sup>2</sup>). Part of the permalloy film was left unpatterned and used as reference sample for the BLS measurements. Further details of the fabrication process are described in Ref. 11. The nanowires arrays have uniform width and interwire spacing, as revealed from the scanning electron microscopy (SEM) micrographs of Fig. 1.

The hysteresis loops were measured using a vectorial magneto-optical Kerr effect magnetometry and microscopy (V-MOKE/ $\mu\text{MOKE}$ ) setup, described in detail in Ref. 12. V-MOKE measurements are sensitive to both in-plane components of magnetization, parallel to the external field  $\mathbf{H}$  (longitudinal loop) and orthogonal to it (transverse loop).

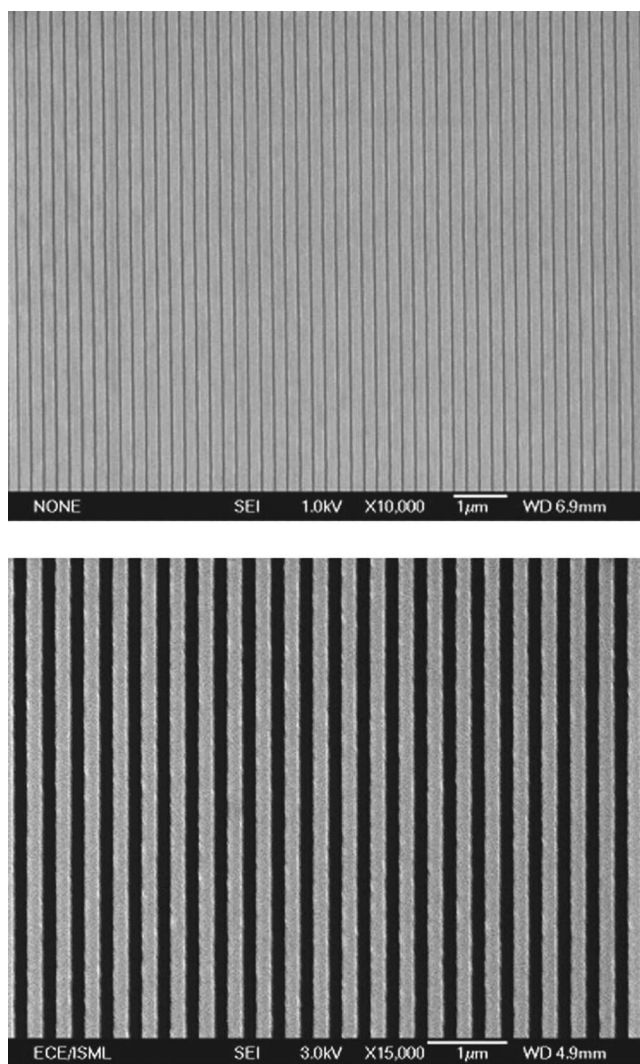


FIG. 1. SEM micrographs of the nanowires arrays with wire width  $w=175$  nm, spacing  $\Delta=35$  nm (upper panel), and  $\Delta=175$  nm (lower panel).

Such a feature allows the reconstruction of the magnetization vector at any step of the magnetization reversal. For investigating the sample along different directions and finding its hard and easy axis, it was rotated about the normal axis to the sample plane. Local hysteresis loops were recorded focusing the laser beam over a circular spot with diameter of about 7  $\mu\text{m}$  ( $\mu\text{MOKE}$ ). This corresponds to illuminate and to measure the hysteresis loops of a reduced number of wires (about 30 wires in the case of the largest spacing).

Brillouin light scattering measurements were carried out at the GHOST laboratory, Perugia University.<sup>13</sup> Monochromatic P-polarized light, from a solid state laser (532 nm line) with a power of about 200 mW, was focused on the patterned area using a camera objective of numerical aperture 2 and focal length 50 mm. Backscattered light was analyzed using a Sandercock type (3+3) pass tandem Fabry-Pérot interferometer.<sup>14</sup> We performed a polarization analysis to minimize the phonon contribution to the spectra. A magnetic field of fixed intensity (0.5 kOe) was applied along the easy direction of the wires, i.e. along their length and perpendicu-

lar to the scattering plane of light. BLS spectra were recorded by varying the incidence angle of light with respect to the sample normal in the range between  $10^\circ$  to  $70^\circ$ . This corresponds to change the spin-wave wave number ( $k$ ) parallel to the sample from  $0.41 \times 10^5$  to  $2.22 \times 10^5 \text{ cm}^{-1}$ .

From the frequency dispersion of the Damon-Eshbach mode<sup>15</sup> in the continuous unpatterned permalloy film, the values of the saturation magnetization  $4\pi M_s = 8.1 \text{ kOe}$ , and of the gyromagnetic ratio  $\gamma/(2\pi) = 2.93 \text{ GHz/Oe}$ , have been derived. These parameters have been used to calculate the spin-wave frequency dispersion according to the theoretical model described in the next paragraph.

### III. THEORY

The results of the calculation presented here are based on the theory developed previously.<sup>16</sup> In Ref. 16 a plane structure having an infinite number of parallel wires of infinite length was considered. The structure is periodical in the direction  $x$ , which is perpendicular to the wire length. The period of the structure is  $T = w + \Delta$ . The theoretical analysis was based on solution of the linearized Landau-Lifschitz magnetic torque equation (LLE). To make the problem one-dimensional a commonly used procedure of averaging of all the dynamic components of the equation over the wire thickness  $L$  (see, e.g., Ref. 17) was utilized.

The solution describing a traveling wave on a periodic structure was sought in the form of Bloch waves

$$m_{kn}(x) = \tilde{m}_{kn}(x) \exp(ikx), \quad (1)$$

where  $k$  is a small wave vector taking on continuous values and  $m_{kn}(x)$  is a spatially periodic function with the period  $T$ ,  $\tilde{m}_{kn}(x + jT) = \tilde{m}_{kn}(x)$ . Here  $n$  is a collective mode number, and  $j$  is an integer.

The dipolar field of the magnetization distribution (1) was calculated by using the Green's function approach. The condition that for the eigenwaves of the structure the profile of dipolar field should coincide to a factor with the profile of their dynamic magnetization resulted in an eigenvalue problem for the integral operator of dipolar field

$$\lambda \tilde{m}_j(x) = \sum_{j'=-\infty}^{j'=\infty} \int_{-1/2}^{1/2} P(x, x' + (j' - j)T) \times \exp\{[ik(x' - x + (j' - j)T)]\} \tilde{m}_{j'}(x') dx', \quad (2)$$

where

$$P(x, x') = \frac{1}{p} \ln \frac{(x - x')^4}{[p^2 + (x - x')^2]^2}. \quad (3)$$

In the last expression,  $p$  is the so-called aspect ratio,  $p = L/w$ .

To obtain the eigenfrequency of  $n$ th collective mode, in LLE one should substitute the dipolar field of wires with  $\lambda_n m_j(x)$ , where  $\lambda_n$  is the  $n$ th eigenvalue of (2). This results in an algebraic equation, as follows:

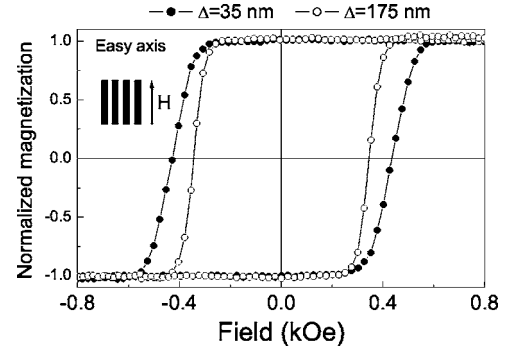


FIG. 2. Comparison between the longitudinal easy axis hysteresis loops measured for the two wires arrays with different spacings. Full (open) points are for the  $\Delta = 35 \text{ nm}$  ( $\Delta = 175 \text{ nm}$ ) spaced wires, respectively.

$$(\omega_n)^2 = \omega_H(\omega_H + \omega_M) - \omega_M^2 \left[ \frac{\lambda_n}{4\pi} + \left( \frac{\lambda_n}{4\pi} \right)^2 \right], \quad (4)$$

where  $\omega_H = \gamma H$ ,  $\omega_M = 4\pi\gamma M_s$ ,  $H$  is the applied static magnetic field,  $M_s$  is the saturation magnetization of the wires, and  $\gamma$  is the gyromagnetic ratio. In the present work we used a numerical solution of the eigenvalue problem (2) for calculation of the spectrum of eigenmodes of the structures.

### IV. RESULTS AND DISCUSSION

The longitudinal V-MOKE hysteresis loops taken from the two samples, without focusing the laser beam, are shown in Figs. 2 and 3. The loops measured with  $H$  parallel to the wires length (easy direction) are plotted in Fig. 2, while those recorded applying  $H$  along the wires width (hard direction) are displayed in Fig. 3, together with the magnetization component perpendicular to the applied field (transverse loops). No transverse component was observed in the correspondence of the  $H$  parallel to the easy direction. The comparison between the easy loops in Fig. 2 gives evidence that the reduction of the interwire distance has no appreciable

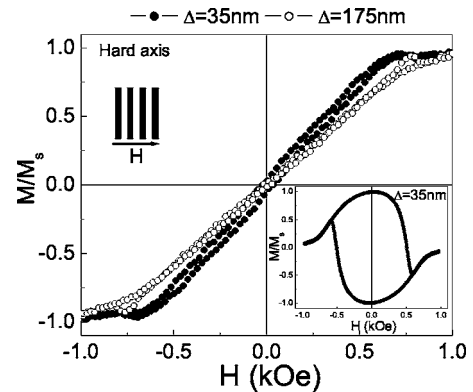


FIG. 3. Comparison between the longitudinal hard axis hysteresis loops measured for the two wires arrays with different spacings. Full (open) points are for the  $\Delta = 35 \text{ nm}$  ( $\Delta = 175 \text{ nm}$ ) spaced wires, respectively. The inset shows the transversal magnetization curve for the  $\Delta = 35 \text{ nm}$  spaced wires.

effect on the onset of the magnetization reversal process, while the slope of the reversal portion of the loops is strongly affected. In particular, the applied field range required for the magnetization reversal of the sample is substantially wider when the interwire distance is decreased. These results can be interpreted as follows: the reversal is initiated by the switching of the magnetization in those wires where the energy barrier for its nucleation is lower because of the presence of defects and irregularities. The presence of the dipolar interaction, which favors the antiparallel orientation of the magnetization of nearest neighboring wires, should anticipate the reversal onset, but if the role of defects in the wires is dominating, negligible variation of the reversal nucleation field is expected when comparing the cases of noninteracting and interacting wires. The effects of dipolar interaction are expected to influence the way in which the magnetization reversal proceeds after the initial stage. If the dipolar interaction is lower or negligible as in the case of wires with larger separation, the reversal of each wire is determined by its own reversal energy barrier and the range of  $H$  required to complete the magnetization reversal substantially reflects the reversal nucleation fields distribution in the probed area of the sample (typically a few  $\text{mm}^2$ ). In the case of wires closer to each other, the non-negligible dipolar interaction, stabilizes the magnetization of the two wires nearest to those that have already switched their magnetization. The magnetization reversal of the two wires nearest to those already reversed will require higher  $H$  values, resulting in a less steep slope of the hysteresis loop and, thus, to a wider range of  $H$  in order to complete the magnetization reversal of the probed area (*viz.*, of the whole sample). In this case the interval of  $H$  required to complete the reversal reflects the interplay between the reversal nucleation field distribution and the effects of the dipolar interaction.

The hysteresis loops recorded by applying  $H$  along the width of the wires, Fig. 3, show an appreciable lowering of the saturation field for the nearest interacting wires as compared to the isolated ones. The lower saturation field observed in the interacting wires can be explained as due to the effect of the dipolar coupling between the structures. In this case, the magnetic charges created along the lateral edges of the wires induce a field in the same direction as the applied field and, hence, the effective demagnetizing field in each wire is reduced.

The behavior of the magnetization component perpendicular to  $H$  (transverse loop), shown in the inset of Fig. 3 for the 35 nm spaced wires (a similar loop shape is obtained for the 175 nm spaced wires), shows that for both samples the magnetization of all wires rotates in the same direction, toward the wires' length direction, as  $H$  is reduced to zero. This is demonstrated by the fact that the transverse component normalized to the magnetization saturation value reaches the maximum value of 1 at zero external field (*viz.*, the magnetization in all the wires is parallel to the wires length and pointing along the same direction). Such a behavior is traceable to a slight misalignment between  $H$  and the direction parallel to wires' width, so that the small component of  $H$  along the wires' length direction biases the rotation of the magnetization of each wire toward the same direction. We rotated the samples about their normal in steps of frac-

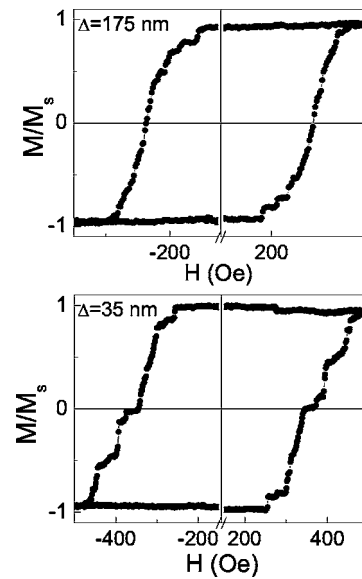


FIG. 4. Measured  $\mu$ MOKE easy axis magnetization curves for the two arrays of wires with different spacings,  $\Delta=175$  nm (upper panel) and  $\Delta=35$  nm (lower panel), respectively.

tions of degree in order to try to observe a different magnetic behavior, but we never succeeded in observing an antiparallel orientation of magnetization at zero field, which would result in a vanishing transverse component of magnetization in the transverse loops, as expected in the case of  $H$  exactly applied perpendicular to the length of dipolar interacting wires. This is not surprising, since experimentally it is practically impossible to achieve a perfect alignment between  $H$  and the samples' structures.

To gain more insight into the reversal process of the two samples, we performed MOKE measurements by focusing the laser beam over a spot with a diameter of  $\sim 7 \mu\text{m}$ . The loops recorded applying  $H$  parallel to the wires length (easy direction) are shown in Fig. 4. The steps visible in both the loops evidence that the reversal is occurring through the separate switching of either individual wires or groups of a few wires. Since, however, the most likely reversal mechanism in this system is a domain wall nucleation and propagation process, in principle, the steps could also be due to domain wall pinning and the formation of domain structures in the wires, such as, *e.g.*, head-to-head and tail-to-tail structures. A strong hint that the steps are due to magnetization switching of at least an individual wire comes from the evaluation of the height of the smallest steps observable in the loop recorded from the sample with largest wires spacing (Fig. 4, upper panel). Such height is about  $\frac{1}{30}$  of the total MOKE signal determined by the magnetization reversal, consistent with the switching of a single wire among the about 30 wires illuminated by the laser spot. This suggests that once the domain walls nucleate they rapidly propagate across the wire, determining a sudden switching of the magnetization of the individual structure. Such a reversal process has been observed in the loops from systems made by a few number of wires, as reported in Refs. 18 and 19. The wide plateau at  $M \approx 0$  displayed by the loop recorded from the sample with the wires closest to each other ( $\Delta=35$  nm),



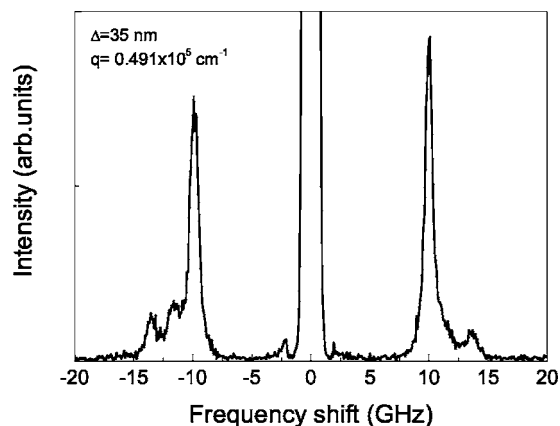


FIG. 5. Typical BLS spectrum for the array of wires with spacing  $\Delta=35$  nm measured for an applied field of 0.5 kOe and wave number  $k=0.41 \times 10^5$  cm<sup>-1</sup>.

which is not present in the loop of the other sample, can be ascribed to the effects of the dipolar interaction which stabilizes the intermediate state characterized by a predominant antiparallel alignment of magnetization of the nearest neighboring wires. Dipolar interaction is also responsible for the larger magnetic field, which is necessary to apply in order to saturate the  $\Delta=35$  nm spaced wires. Due to the magneto-static interaction, the system creates a closure path for the magnetic stray field in adjacent wires, which reduces the overall energy of the system. Then at somewhat higher applied field (Zeeman energy), the system is forced out of this potential well.

Concerning the dynamical properties, Fig. 5 shows a typical BLS spectrum for the nanowire arrays with smaller spacing  $\Delta=35$  nm; a similar spectrum has been measured for wires with larger spacing. We notice that, instead of the single peak corresponding to the Damon-Eshbach mode observed in the continuous reference film, there are three well resolved peaks. They are related to the discretization of the magnetic excitations due to the lateral confinement within the wires width. For the sample with  $\Delta=175$  nm, all the observed peaks are dispersion-free, i.e., their frequency does not change over the entire whole range of wave numbers investigated, as seen in the upper panel of Fig. 6. On the contrary, for wires placed at small distances from each other ( $\Delta=35$  nm), lower panel of Fig. 6, the frequency of the lowest mode, which has the largest intensity in the BLS spectrum, has a pronounced dispersive character. The presence of such a dispersion is the main evidence of wire coupling. Notice that the measured frequencies are well reproduced by our calculations (continuous curves), including the lowest dispersive mode of the 35 nm spaced wires. However, it can be seen that the experimentally measured dispersion is smaller than the calculated one. A possible reason for this is that in the calculation we did not take into account the magnetic damping. The damping determines the propagation length of traveling collective modes and thus the number of neighboring wires which are coupled by the dipole interaction. The decrease of the number of coupled neighbors may result in the decrease of the dispersion. For example, Fig. 2 in Ref. 16 demonstrates the frequency ranges of existence of

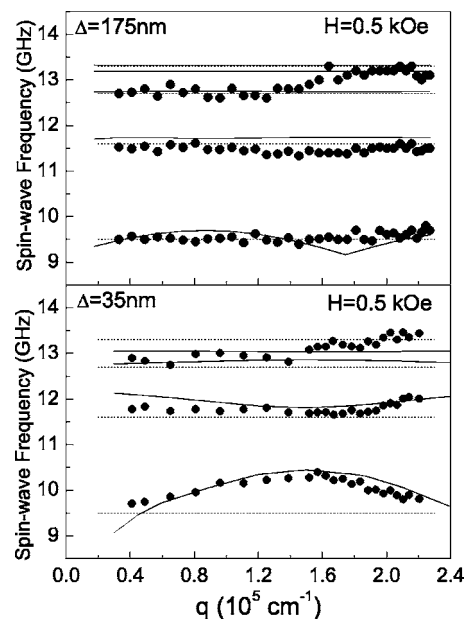


FIG. 6. Experimental and calculated dispersion of the spin-wave frequency modes for an infinite array of permalloy wires with thickness of 20 nm and width  $w=175$  nm. The wires spacing are  $\Delta=175$  nm (upper panel) and  $\Delta=35$  nm (lower panel), respectively. The continuous curves were calculated using the theoretical model described in the text. Dotted lines are the calculated frequencies for the resonant spin modes for an isolated wire.

the lowest collective standing mode on a structure consisting of only 3 parallel wires and that traveling on the periodic array of infinite length of the same wires with the same interwire distance. (No damping was taken into account.) The frequency width of the spectrum in the first case is considerably smaller, confirming that there exists a dependence of the frequency spectrum width and the number of coupled wires.

Now let us briefly discuss the character of collective mode dispersion, starting with the mode profile dependence on the strength of dipolar coupling. We will consider the in-plane component of the dynamic magnetization,  $m_x$ . Due to a huge ellipticity of precession of the magnetization vector in permalloy, this component is much larger than the out-of-plane one. Therefore it mainly contributes to the dynamic dipole (stray) field each wire induces in the array plane outside the wire itself.

First we discuss the asymptotical behavior of eigenprofiles of dynamic magnetization through the array  $m_x(x)$  when the distance between the neighboring wires tends to zero. It will help us to understand the system behavior in the case of large dipole coupling of wires. It is obvious that for  $k=0$ , the case of homogeneous magnetization precession in an unstructured film is asymptotically recovered. In the case  $k=\pi/T$  the profile tends to that sinusoidal of usual Damon-Eshbach (DE) wave in an unstructured film.<sup>15</sup> The wave number of the wave is  $k_{DE}=\pi/T$ .

Turn now to the case of the nonvanishing interwire distance. Figure 7 shows calculated profiles of distribution of dynamic magnetization through the wire width for the the lowest collective mode. The profiles are plotted for both ex-

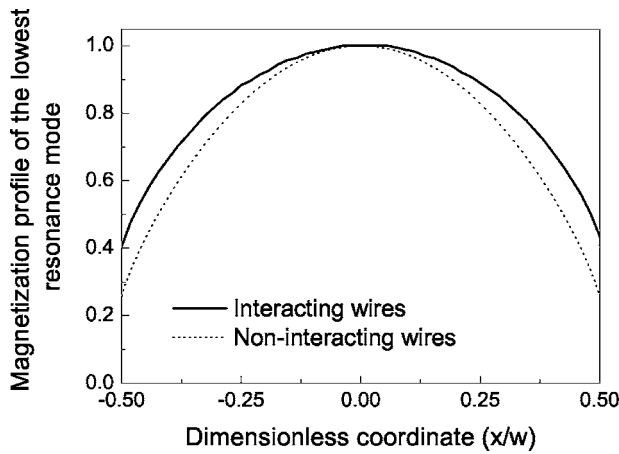


FIG. 7. Comparison between the distributions of dynamic magnetization for the lowest frequency mode in the case of interacting ( $\Delta=35$  nm, continuous curve) and quasi-isolated noninteracting ( $\Delta=175$  nm, dotted curve) wires. The dimensionless coordinate in abscissa is normalized to the wire width  $w$ .

perimental distances between the neighboring wires,  $\Delta = 35$  nm and  $\Delta = 175$  nm. The case under consideration,  $k = 0$ , corresponds to the lowest frequency boundary of the first Brillouin zone for the mode. The condition,  $k = 0$ , physically means that all the wires on the array precess in phase. The in-phase precession favors directing the force lines of the dynamic dipole field of any individual wire to the neighboring wire, contrary to the case of uncoupled wires, where they close through the wire itself in the opposite direction to  $m_x$ . Directing the force lines opposite to  $m_x$  results in a decrease of the dipolar field near the wire boundaries. Since the eigenprofile of dynamic magnetization should follow that of the dipole field, this results in an effective dipolar pinning of  $m_x$  at the wire edges. This is clearly seen in Fig. 7 (dotted line) where calculations show that the profile coincides with that for the lowest resonance in an uncoupled wire with the graphical accuracy.

If the force lines are partly directed into the neighboring wires, the dipole field near the wire edges increases. As a result, the amplitude of magnetization precession at the edges increases, implying a smaller effective pinning of the dynamic magnetization due to coupling (Fig. 7, solid line). The profile of dynamic magnetization through the whole array becomes more homogeneous, than in the case of a small or absent coupling. As a result, the eigenfrequency becomes closer to the frequency of the homogeneous precession of an unstructured film. This means that the eigenfrequency shifts down.

In the case of the upper boundary of the Brillouin zone,  $k = \pi/T$ , the magnetization vector in neighboring wires precess in antiphase. Therefore for the lowest mode the directions of  $m_x$  in neighboring wires are now opposite, which forces directing the force lines of the dipole field within each wire itself opposite to  $m_x$ . The dipole energy associated with this state is larger than that associated with an uncoupled wire, since the contradirected fields of the neighboring wires “repulse” each other. This leads to an increase of effective dipolar pinning of the  $m_x$  at the wire edge, which is clearly

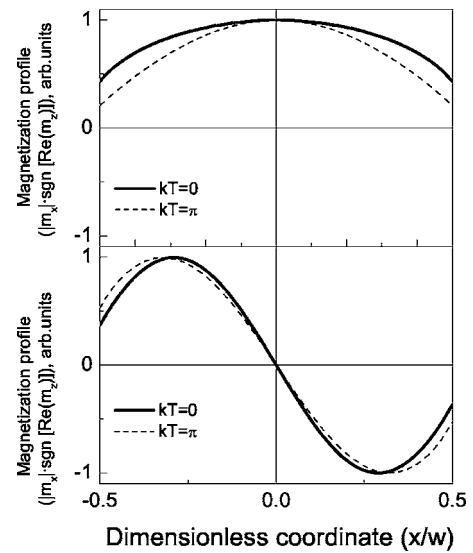


FIG. 8. Comparison between the calculated profile of dynamic magnetization for the lowest frequency mode (upper panel) and the next one (lower panel) for  $k=0$  (thick line) and for  $kT=\pi$  (thin line). Wires separation is  $\Delta=35$  nm. The dimensionless coordinate in abscissa is normalized to the wire width  $w$ .

seen in Fig. 8 (upper panel). As a result, the overall profile of dynamic magnetization through the whole array becomes closer to that of the traveling DE wave with the wave number  $\pi/T$  in an unstructured film. Therefore, the frequency gets closer to this value, which is larger than that of the lowest resonance in a separated wire. Thus, in the first Brillouin zone, i.e., between  $k=0$  and  $k=\pi/T$ , the slope of dispersion is positive.

For the next collective mode the situation is quite opposite, which results in a dispersion of opposite sign for this mode. The profiles of  $m_x$  for this modes are shown in Fig. 8 (lower panel). For  $k=0$  all the wires are in phase, this means that the  $m_x$  components in neighboring wires at the edges of the same spacing show in the opposite directions. Therefore their dipole fields “repulse,” and the effective pinning of magnetization at the edges increases. As a result, the eigenfrequency shifts upward compared with the isolated wire. (The distribution of  $m_x$  through the whole array in this case has a shape close to the sinusoidal one with a period  $T$ , therefore the frequency tends to the eigenfrequency of Damon-Eshbach wave with  $k=2\pi/T$  in an unstructured film.)

For  $k=\pi/T$ , the  $m_x$  components in neighboring wires at the edges of the same spacing show in the same direction. This favors directing the force lines to the neighboring wire and results in a decrease of dipolar energy, a decrease of the effective pinning, and a downshift of the eigenfrequency. (The distribution of  $m_x$  through the whole array in this case has a shape to some extent similar to the sinusoidal one with a period  $2T$ , therefore the frequency gets closer to the eigenfrequency of Damon-Eshbach wave with  $k=\pi/T$  in an unstructured film.)

The stray field of this mode outside the wires is much smaller than that of the lowest one, owing to the change of the sign of  $m_x$  across the wire width. The much smaller stray

(dipole) field leads to a much smaller coupling of wires and to a much smaller slope of dispersion curve for this mode compared with the lowest mode. The higher modes have yet more smaller slopes because of yet more smaller stray field because of the larger number of positive and negative half-periods in the distribution  $m_x(x)$  through the wire width.

## V. CONCLUSIONS

We report the observation of magnetostatic coupling in arrays of differently spaced permalloy wires with the same thickness and width. Our results clearly indicate that the switching behavior of the coupled wires is affected by magnetostatic interaction. The magnetic hysteresis curves for the sample with interwire spacing  $\Delta=35$  nm consist of a series of steps followed by plateaus corresponding to stable magnetization configurations related to the antiparallel alignment of wires. In the other sample, where the interwire spacing is 175 nm, the wires can be considered as noninteracting. In this case the magnetization reversal is governed by the distribution of energy barriers for the reversal nucleation, deter-

mined by the morphological defects. The MOKE results were qualitatively reproduced by means of micromagnetic simulations.

Concerning the dynamical properties, in the case of magnetostatic coupled wires, we measured a dispersive character of the lowest frequency mode instead of the dispersion-free behavior of the resonant modes in uncoupled wires. This experimental evidence is in agreement with the predictions of a theoretical model which considers the presence of collective modes in the wires array.

## ACKNOWLEDGMENTS

The work was partly supported by the Italian Ministero Istruzione, Università e Ricerca (PRIN 2003025857 and FIRB RBNE017XSW), by the Russian Foundation for Basic Research, Grant No. 05-02-17714, and by the French Ministry of Education and Research (project ACI "NANODYNE" NR0095). One of us (M.K.) acknowledges financial support from the Australian Research Council. We are also grateful to Dr. Y. Roussigné for a helpful discussion.

---

\*Present address: Dipartimento di Fisica, Università degli Studi di Perugia, Via A. Pascoli, 06123 Perugia, Italy. Email address: gubbiotti@fisica.unipg.it

<sup>1</sup>F. J. Himpsel, J. E. Ortega, G. J. Mankey, and R. F. Willis, *Adv. Phys.* **47**, 511 (1998); *Magnetic Nanostructures*, ed. By H. S. Nalwa (American Scientific Publishers, Los Angeles, 2002).

<sup>2</sup>J. I. Martín, J. Nogues, Kai Liuc, J. L. Vicente, and I. K. Schuller, *J. Magn. Magn. Mater.* **256**, 449 (2003), and references therein.

<sup>3</sup>R. P. Cowburn, A. O. Adeyeye, and M. E. Welland, *New J. Phys.* **1**, 16.1 (1999).

<sup>4</sup>R. P. Cowburn, *J. Phys. D* **33**, R1 (2000).

<sup>5</sup>J. Shibata, K. Shigeto, and Y. Otani, *Phys. Rev. B* **67**, 224404 (2003).

<sup>6</sup>V. Novosad, M. Grimsditch, K. Yu. Guslienko, P. Vavassori, Y. Otani, and S. D. Bader, *Phys. Rev. B* **66**, 052407 (2002).

<sup>7</sup>V. Novosad, K. Yu. Guslienko, H. Shima, Y. Otani, S. G. Kim, K. Fukamichi, N. Kikuchi, O. Kitakami, and Y. Shimada, *Phys. Rev. B* **65**, 060402(R) (2002).

<sup>8</sup>R. Arias and D. L. Mills, *Phys. Rev. B* **67**, 094423 (2003).

<sup>9</sup>Z. K. Wang, M. H. Kuok, S. C. Ng, D. J. Lockwood, M. G. Cottam, K. Nielsch, R. B. Wehrspohn, and U. Gösele, *Phys. Rev. Lett.* **89**, 027201 (2002).

<sup>10</sup>C. Mathieu, C. Hartmann, M. Bauer, O. Buettner, S. Riedling, B. Roos, S. O. Demokritov, B. Hillebrands, B. Bartenlian, C. Chappert, D. Decanini, F. Rousseaux, E. Cambri, A. Müller, B. Hoffman, and U. Hartmann, *Appl. Phys. Lett.* **70**, 2912 (1997).

<sup>11</sup>N. Singh, S. Goolaup, and A. O. Adeyeye, *Nanotechnology* **15**, 1539 (2004).

<sup>12</sup>P. Vavassori, *Appl. Phys. Lett.* **77**, 1605 (2000).

<sup>13</sup><http://ghost.fisica.unipg.it>

<sup>14</sup>J. R. Sandercock, in *Light Scattering in Solids III*, edited by M. Cardona and G. Güntherodt (Springer-Verlag, Berlin, 1982), p. 173.

<sup>15</sup>R. W. Damon and J. R. Eshbach, *J. Phys. Chem. Solids* **19**, 308 (1961).

<sup>16</sup>M. P. Kostylev, A. A. Stashkevich, and N. A. Sergeeva, *Phys. Rev. B* **69**, 064408 (2004).

<sup>17</sup>K. Yu. Guslienko, S. O. Demokritov, B. Hillebrands, and A. N. Slavin, *Phys. Rev. B* **66**, 132402 (2002).

<sup>18</sup>J. Velázquez, C. Garcia, M. Vázquez, and A. Hernando, *Phys. Rev. B* **54**, 9903 (1996).

<sup>19</sup>M. Knobel, L. C. Sampaio, E. H. C. P. Sinnecker, P. Vargas, and D. Altbir, *J. Magn. Magn. Mater.* **249**, 60 (2002).